

Invariant manifolds in Celestial Mechanics

E. Barrabés Vera

Universitat de Girona

Jornada de Sistemes Dinàmics a Catalunya



Outline

Introduction

A paradigmatic model

The circular RTBP

Invariant manifolds

Other manifolds

Interplanetary networks

Space mission design

Natural phenomena

Other models

Bicircular

Parabolic

Other models



The comprehension of simple models allows both to understand the mechanisms that explain natural phenomena and to design spacecraft mission.



The comprehension of simple models allows both to understand the mechanisms that explain natural phenomena and to design spacecraft mission.

All models are wrong, but some are useful.

George E. P. Box (1918–2013)

Outline

Introduction

A paradigmatic model

The circular RTBP

Invariant manifolds

Other manifolds

Interplanetary networks

Space mission design

Natural phenomena

Other models

Bicircular

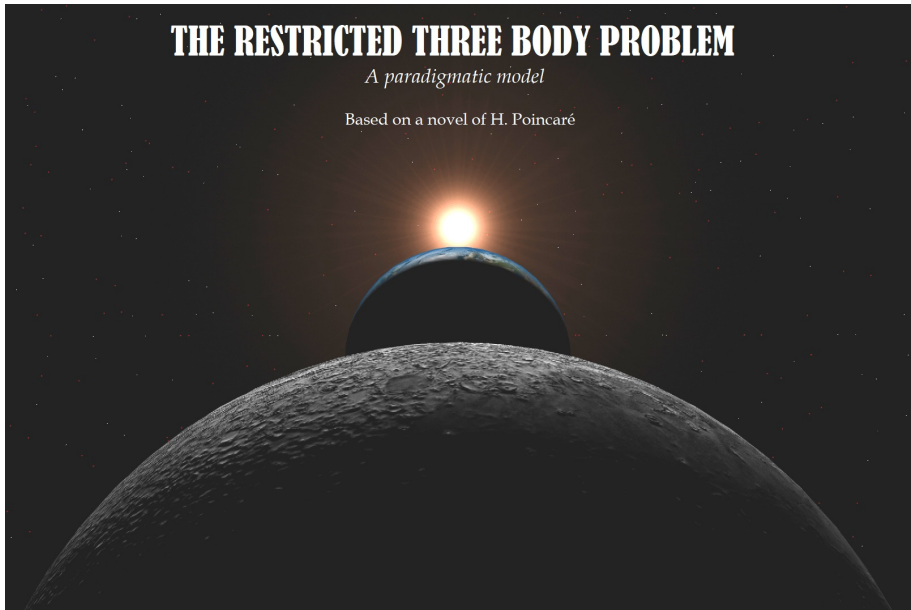
Parabolic

Other models

THE RESTRICTED THREE BODY PROBLEM

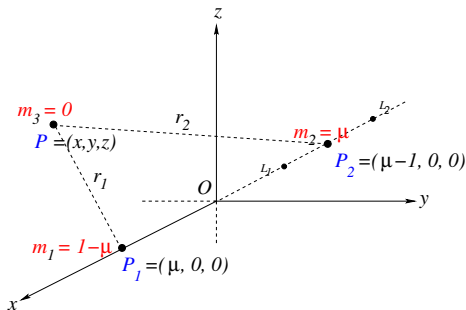
A paradigmatic model

Based on a novel of H. Poincaré



The Circular Restricted Three Body Problem

The motion in a rotating system of a (massless) particle under the gravitational attraction of two main bodies (primaries) moving in a circular orbit



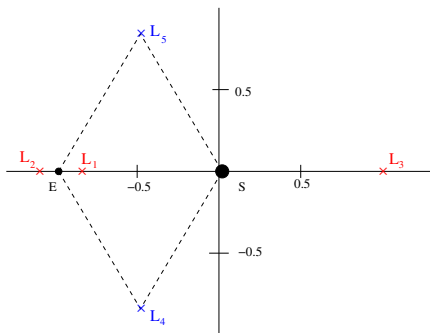
$$H(x, y, z, p_x, p_y, p_z) = \frac{1}{2}(p_x^2 + p_y^2 + p_z^2) - xp_y + yp_x - \frac{1 - \mu}{r_1} - \frac{\mu}{r_2},$$

$$r_1 = \sqrt{(x - \mu)^2 + y^2 + z^2}, \quad r_2 = \sqrt{(x - \mu + 1)^2 + y^2 + z^2}.$$

Planar Circular Restricted Three Body Problem (CRTBP)

Equilibrium points:

- L_1, L_2, L_3 collinear points
- L_4, L_5 triangular points



Energy (Jacobi constant):

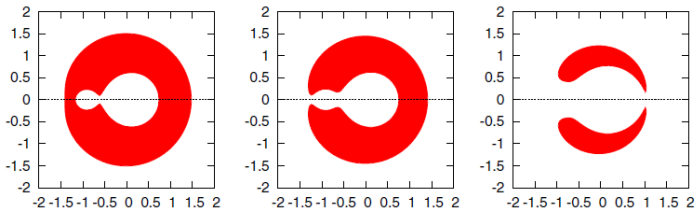
$$C_J = -2h = x^2 + y^2 + 2\frac{1-\mu}{r_1} + 2\frac{\mu}{r_2} + \mu(1-\mu) - v^2$$



Hill's region

For a fixed value of the energy, the zero velocity curves (surfaces) enclosed the Hill's regions where the motion is allowed.

$$v^2 = x^2 + y^2 + 2\frac{1-\mu}{r_1} + 2\frac{\mu}{r_2} + \mu(1-\mu) - C_J \geq 0$$



Configuration space (x, y)

Dynamics around the equilibrium points

- The **triangular points**, $L_{4,5}$, are linearly stable for small values of the mass parameter
- The **collinear points**, L_i , $i = 1, 2, 3$ are unstable:

$$\text{Spec}(D\mathbf{f}(L_i)) = \{\lambda, -\lambda, i\omega_v, -i\omega_v, i\omega_p, -i\omega_p\},$$

Linear:

$\pm\lambda$

saddle

×

$\pm i\omega_p$

center

×

$\pm i\omega_v$

center

↑

↑

Non-linear:

inv. manif.

planar p.o.

vertical p.o.

Cantor set of 2D tori

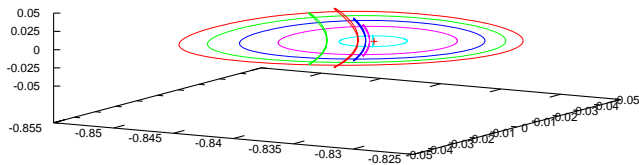


Dynamics around the equilibrium points

- The **triangular points**, $L_{4,5}$, are linearly stable for small values of the mass parameter
- The **collinear points**, L_i , $i = 1, 2, 3$ are unstable:

$$\text{Spec}(D\mathbf{f}(L_i)) = \{\lambda, -\lambda, i\omega_v, -i\omega_v, i\omega_p, -i\omega_p\},$$

At each energy level $H = h \exists$ one planar and one vertical periodic orbits (Lyapunov p.o.). Along the families, bifurcations appear (halo orbits).

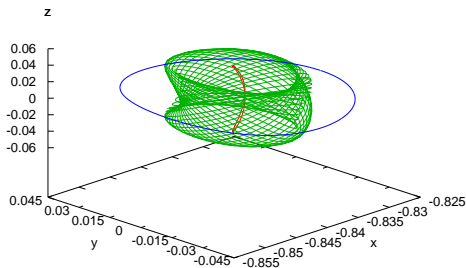


Dynamics around the equilibrium points

- The **triangular points**, $L_{4,5}$, are linearly stable for small values of the mass parameter
- The **collinear points**, L_i , $i = 1, 2, 3$ are unstable:

$$\text{Spec}(D\mathbf{f}(L_i)) = \{\lambda, -\lambda, i\omega_v, -i\omega_v, i\omega_p, -i\omega_p\},$$

At each energy level $H = h \exists$ a family of quasi-periodic orbits (inv. tori)



Invariant manifolds in CRTBP

For X an unstable invariant object (equilibrium point, periodic or quasi periodic orbit):

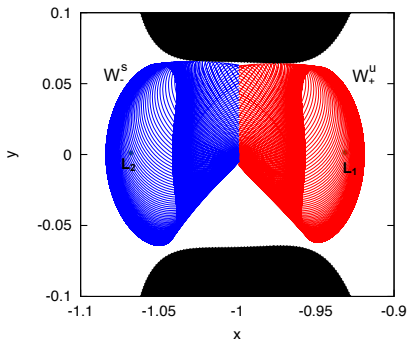
$$W^u(X) = \{\mathbf{q} \in \mathbb{R}^6 \mid \lim_{t \rightarrow -\infty} d(\phi_t(\mathbf{q}), X) = 0\},$$

$$W^s(X) = \{\mathbf{q} \in \mathbb{R}^6 \mid \lim_{t \rightarrow +\infty} d(\phi_t(\mathbf{q}), X) = 0\},$$

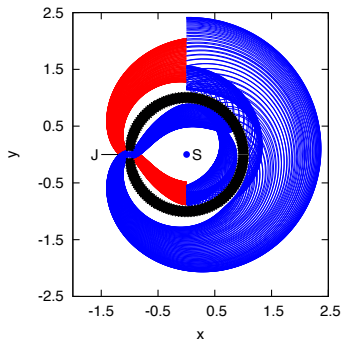
where ϕ_t is the flow and $d(\phi_t(\mathbf{q}), X)$ is the distance between $\phi_t(\mathbf{q})$ and X .

Invariant manifolds in CRTBP

Typical behavior of right $W_+^{u/s}$ and left $W_-^{u/s}$ branches associated to planar Lyapunov orbits around L_1 and L_2



Secondary's region

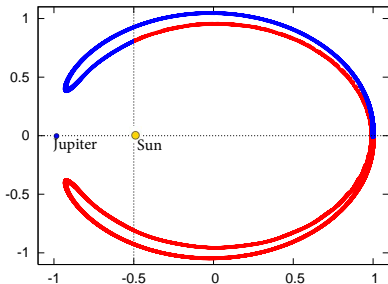
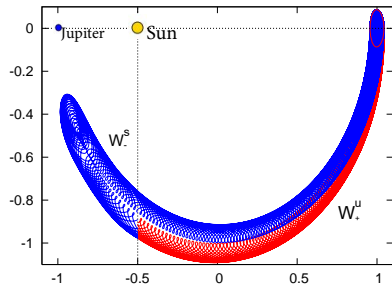


Outer and inner regions

Configuration space (x, y)

Invariant manifolds in CRTBP

Typical behavior of right $W_+^{u/s}$ and left $W_-^{u/s}$ branches associated to planar Lyapunov orbits around L_3



Configuration space (x, y)

Homoclinic and heteroclinic orbits

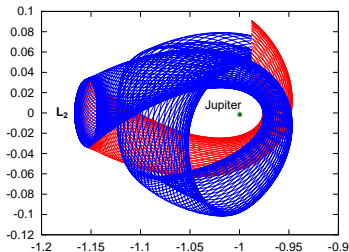
If there exists a transversal intersection of the stable and unstable i.m., the dynamics of the nearby orbits is complex and rich

- \exists a homo/heteroclinic connection: orbit that tends forward ($t \rightarrow +\infty$) and backward ($t \rightarrow -\infty$) to the hyperbolic object X/Y
- existence of infinitely many periodic orbits close to it (and performing a similar path)
- existence of homoclinic connections of *higher* order

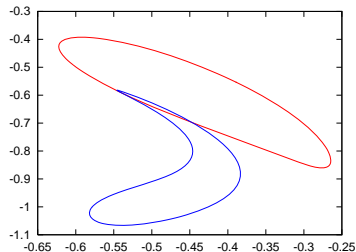
Homoclinics to planar Lyapunov orbits around $L_{1,2}$

For a fixed energy h , a planar Lyapunov orbits OL_i , $i = 1, 2, 3$, and a fixed section Σ

- $W^{u/s}(OL_i)$ are 2-dimensional (tubes)
- $W^{u/s}(X) \cap \Sigma$ are S^1 -like closed curves.



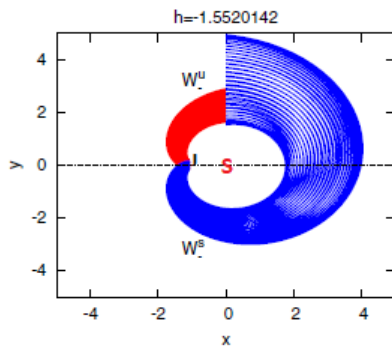
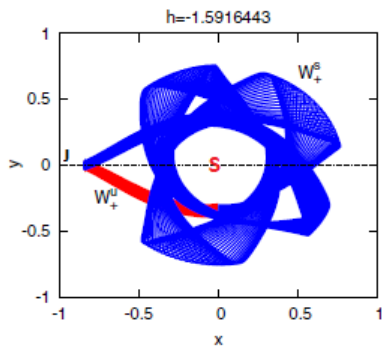
(x, y) -plane



(p_x, p_y) -plane

Homoclinics to planar Lyapunov orbits around $L_{1,2}$

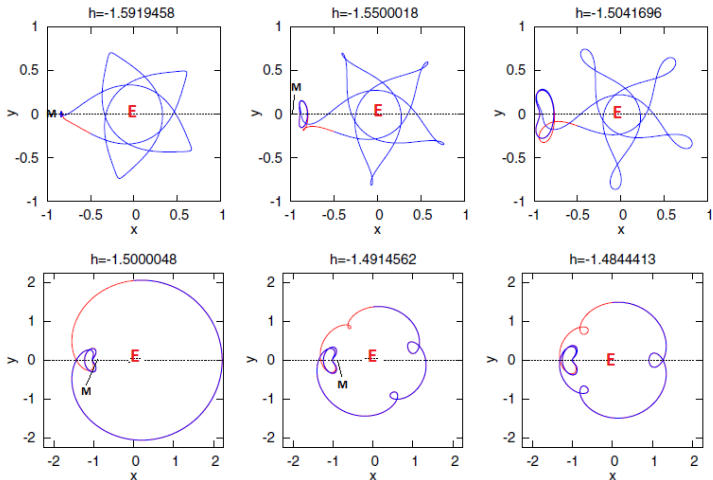
Surrounding the big primary: $W_+^{u/s}(OL_1)$ (left) or $W_-^{u/s}(OL_2)$ (right)





Homoclinics to planar Lyapunov orbits around $L_{1,2}$

Earth-Moon RTBP - homoclinics surrounding the Earth

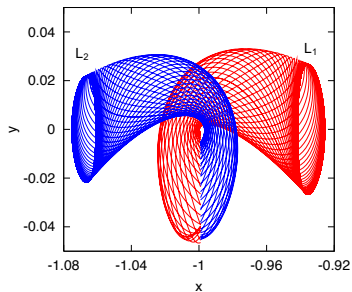




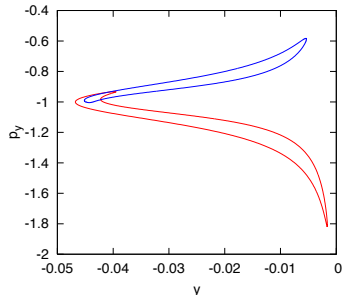
Heteroclinic to Lyapunov orbits around $L_{1,2}$

Heteroclinic connections: $W^u(OL_1) \cap W^s(OL_2)$

Sun - Jupiter CRTBP



(x, y) -plane

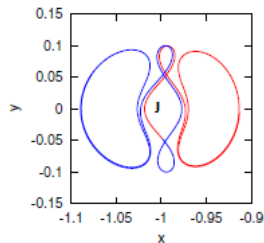
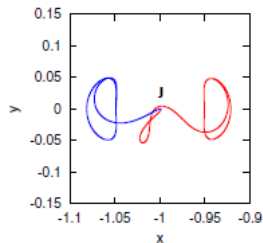
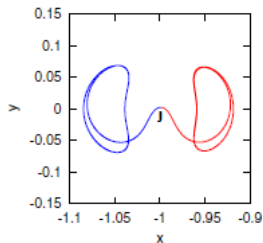


(y, p_y) -plane

Heteroclinic to Lyapunov orbits around $L_{1,2}$

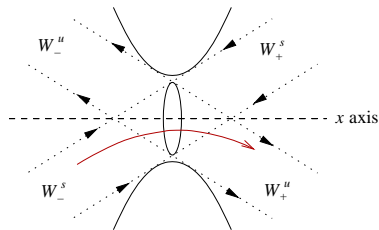
Heteroclinic connections: $W^u(OL_1) \cap W^s(OL_2)$

Sun - Jupiter CRTBP

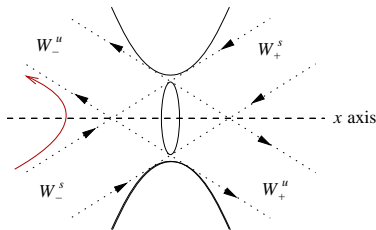


Transit and non-transit orbits in planar CRTBP

A trajectory approaching a p.o., either forward or backward in time from one of the three regions, is considered *transit* if it traverses the bottleneck corresponding to the LPO and goes to the next region



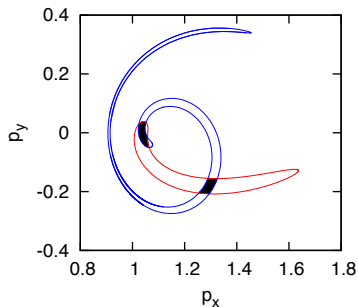
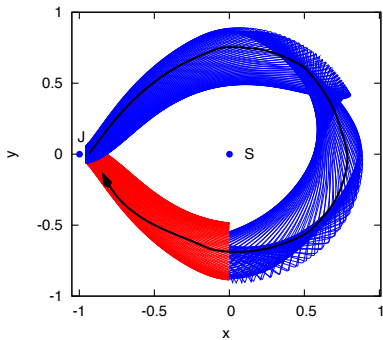
Transit orbit



Non-transit orbit

Transit orbits are known to lie in the *interior* of the invariant manifold tubes of the p.o., that separate them from non-transit orbits (Conley, 1968; McGehee 1969)

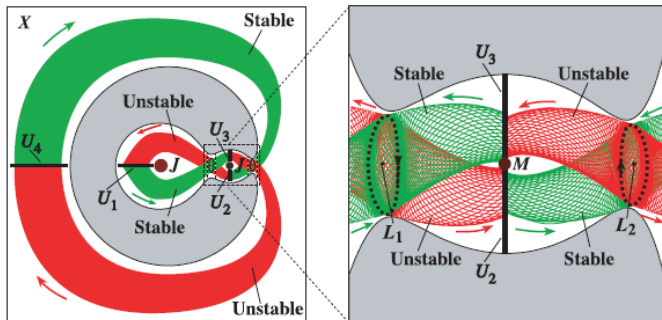
Transit and non-transit orbits in planar CRTBP



Transit from Jupiter region \rightarrow inner region \rightarrow Jupiter region:
the orbits may lie in the interior of both invariant manifolds W^u and W^s

Transit and non-transit orbits in planar CRTBP

Transition chain

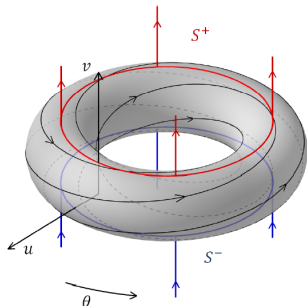


Credits: Gomez et al. Nonlinearity (2004)

Other manifolds

Ejection-Collision Orbit (ECO): the distance between the particle and a primary tends to zero when $t \rightarrow t_0^+$ (ejection) and $t \rightarrow t_1^-$ (collision).

- **Key point:** heteroclinic connections between different equilibrium points living on the **collision manifold** (regularization of the singularity at the primary): a 2-d torus with two circles of equilibrium points



3d invariant manifolds $W^u(S^+)$ ejection orbits , $W^s(S^-)$ collision orbits

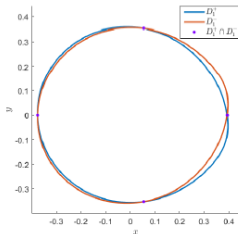
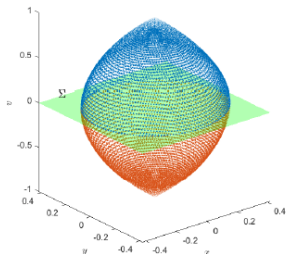
Credits: Ollè, Rodríguez, Soler, CNSNS (2017)



Other manifolds

Ejection-Collision Orbit (ECO): the distance between the particle and a primary tends to zero when $t \rightarrow t_0^+$ (**ejection**) and $t \rightarrow t_1^-$ (**collision**).

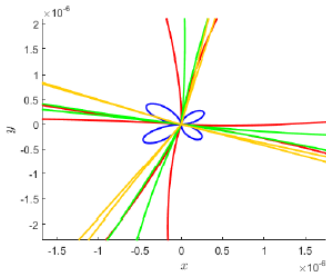
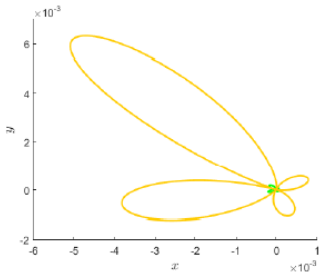
- **Key point:** heteroclinic connections between different equilibrium points living on the **collision manifold** (regularization of the singularity at the primary): a 2-d torus with two circles of equilibrium points



First intersection of $W^u(S^+) \cap \Sigma$, $W^s(S^-) \cap \Sigma$

Credits: Ollè, Rodríguez, Soler, CNSNS (2017)

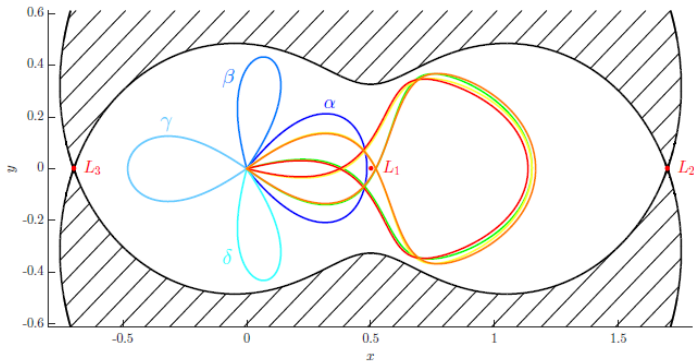
Ejection-Collision Orbit (ECO)



Second intersection of $W^u(S^+) \cap \Sigma$, $W^s(S^-) \cap \Sigma$

Credits: Ollè, Rodríguez, Soler, CNSNS (2017)

Ejection-Collision Orbit (ECO)



ECO for $\mu = 0.5$ and $h = H(L_2)$

Credits: Ollè, Rodríguez, Soler, CNSNS (2017)

Outline

Introduction

A paradigmatic model

The circular RTBP

Invariant manifolds

Other manifolds

Interplanetary networks

Space mission design

Natural phenomena

Other models

Bicircular

Parabolic

Other models

Interplanetary network



Space mission design

- Patched-conic method: Keplerian approximation of a trajectory by linking different trajectories of a chain of two-body problems. The Sun – SC problem is followed until the SC reaches the sphere of influence of a planet.

Planet – Spacecraft \longrightarrow Sun – SC \longrightarrow Planet – SC \longrightarrow ...

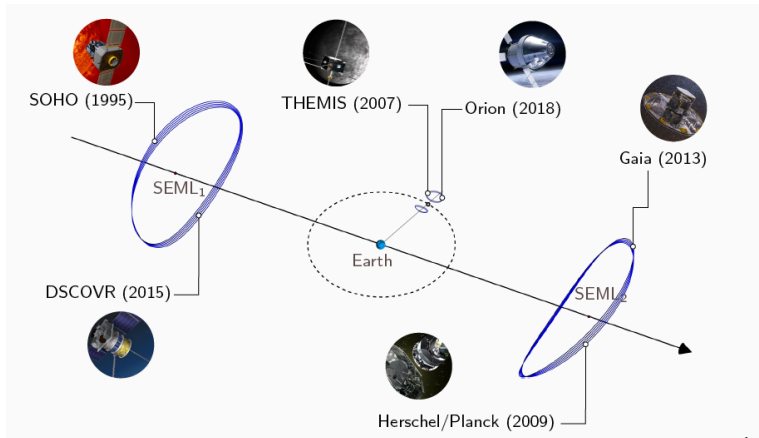
Pioneer (1972), Voyager (1977), Galileo (1989), Mars Observer (1992)

- More demanding missions need better approximations. The Circular RTBP can be used as a (very good) first model to obtain initial seeds that can be refined to obtain solutions in a more complex models.

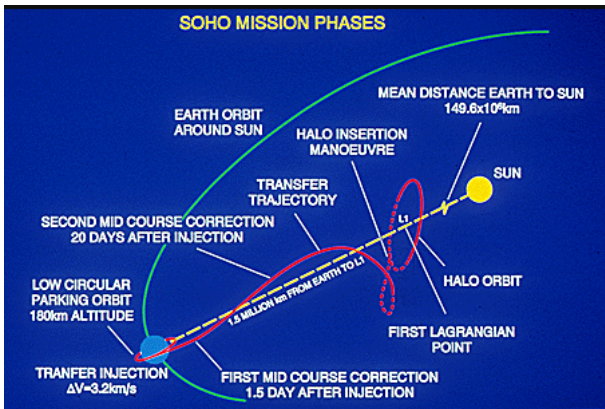
“Low energy transfers” + Δv

Navigation using invariant manifolds and chains of homo/heteroclinic connections.

Libration point orbits missions



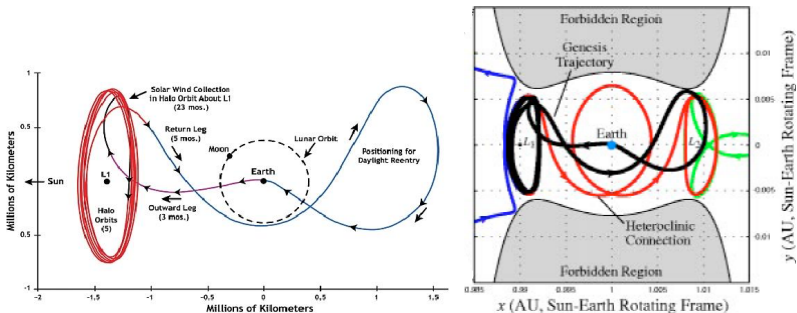
SOHO 1995 – ...



Schematic view of the SOHO transfer to a halo orbit around Sun-Earth's L_1 point.

Genesis 2001-2004

Genesis is considered the first mission designed using modern Dynamical Systems theory.



First approximation chain starting at parking orbit around the Earth:

$$W^s(\Gamma_1) \rightarrow \Gamma_1 \rightarrow W^u(\Gamma_1) \cap W^s(\Gamma_2) \rightarrow W^u(\Gamma_2) \cap E$$

credits: NASA and Koon et al. Chaos (2000)

Artemis 2010

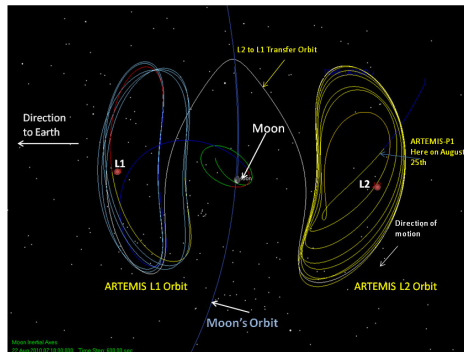
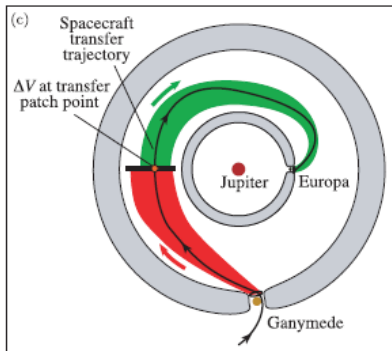
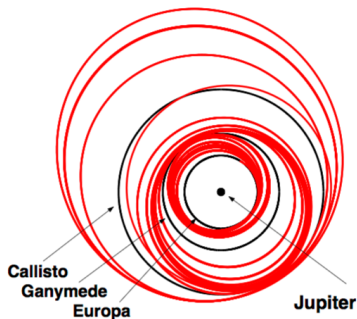


Illustration of ARTEMIS-P1 Librations Orbits credit: NASA GSFC

Mission Themis was launched to Earth-Moon L_2 point in 2007. In 2010 two satellites were reconverted to Artemis mission: one around L_2 while the other was sent to L_1 through a heteroclinic connection.

Low energy tour on Jupiter's Moons

Low Energy Tour of Jupiter's Moons
Seen in Jovicentric Inertial Frame

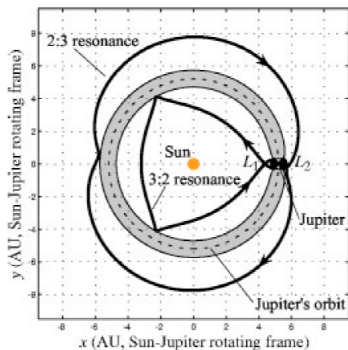


Chain of different CRTPB:

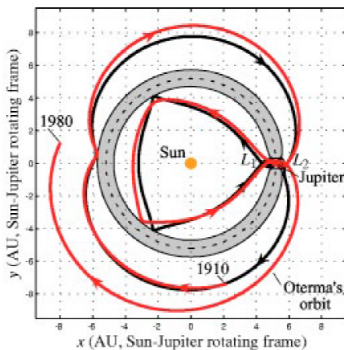
Transfer through $L_{1,2}$ in Jupiter-Ganymede's system – “heteroclinic connection” of i.m. of different systems – transfer through $L_{1,2}$ in Jupiter-Europa's system

Oterma

Oterma follows a trajectory outside Jupiter's orbit close to 2:3 resonance, has a passage through Jupiter's region, and then follows a trajectory inside Jupiter's orbit close to 3:2 resonance



(a)



(b)

Homoclinic to L_1 + homoclinic to L_2

Resonances

Resonances are defined in terms of two body dynamics:

- An elliptic (keplerian) orbit is $p : q$ resonant with Jupiter, if it performs p revolutions around the Sun while Jupiter performs q revolutions.
- The mean motion equals $a^{-3/2} = p/q$, being a the semimajor axis that can be calculated as

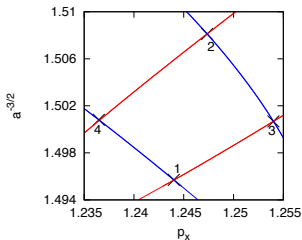
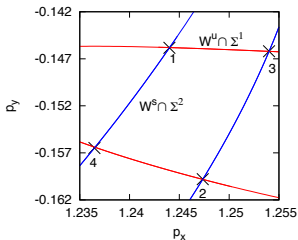
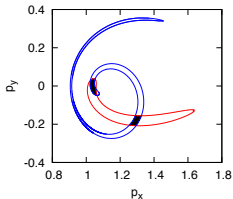
$$a^{-1} = \frac{2}{r} - v^2$$

- For trajectories of the CRTBP that behave essentially as a two-body solution, a will be approximately constant. We can compute its approximate value for the the homoclinics that provide the dynamical chains



Families of homoclinic connections: resonances

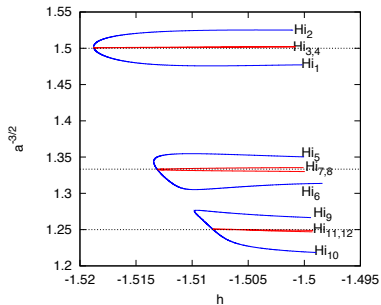
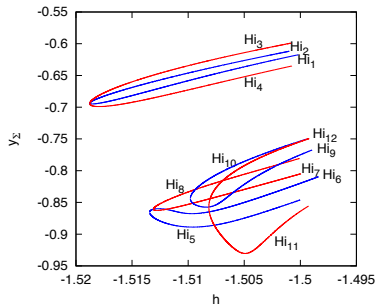
Homoclinic connections to OL_1 in the Sun-Jupiter CRTBP: $W_+^s(OL_1) \cap W_+^u(OL_1)$



Credits: B. Mondelo, Ollè, Nonlinearity (2013)

Families of homoclinic connections: resonances

Families of inner homoclinic connections

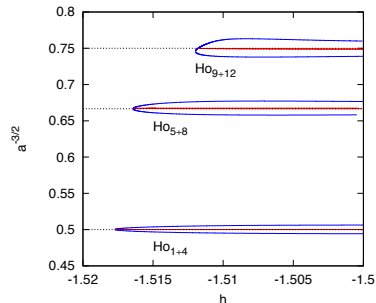
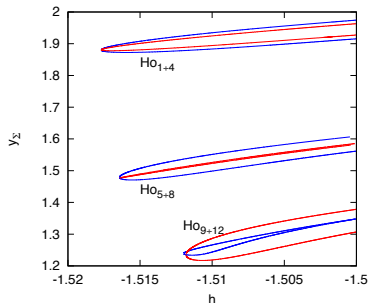


Resonances at 3:2, 4:3, 5:4

Credits: B. Mondelo, Ollè, Nonlinearity (2013)

Families of homoclinic connections: resonances

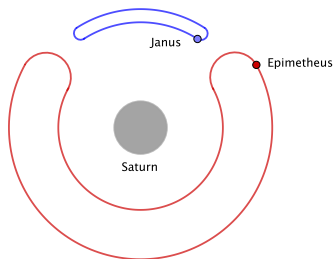
Families of outer homoclinic connections



Resonances at 3:4, 2:3, 1:2

Credits: B, Mondelo, Ollè, Nonlinearity (2013)

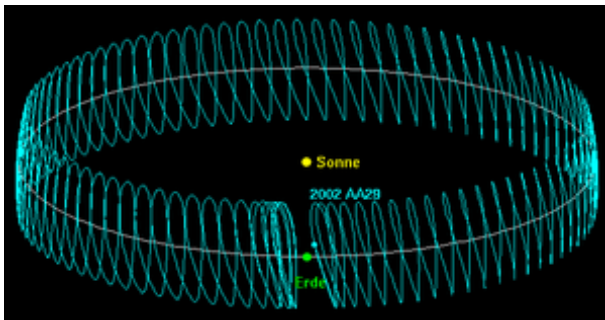
Co-orbital motions



Schematic motion of Janus and Epimetheus around Saturn. Each satellite is shown in a rotating frame.

Credits: NASA-JPL

Co-orbital motions

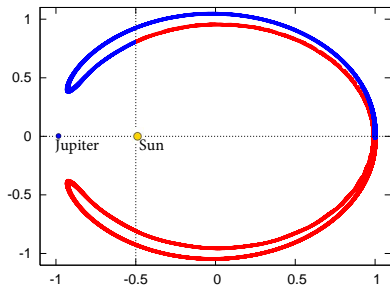
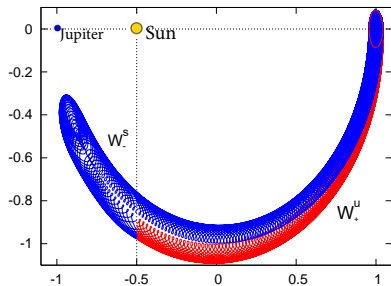


Schematic motion of Earth quasi-satellite 2002 AA29. Co-orbital (horseshoe) motion in Sun-Earth system.

Credits: JPL

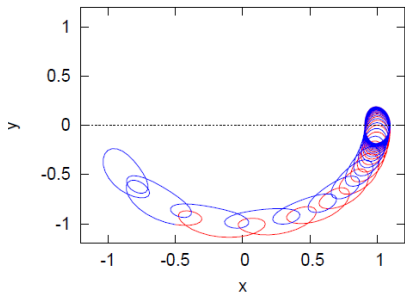
Homoclinics to Lyapunov orbits around L_3

Sun - Jupiter CRTBP - (half) horseshoe-shape homoclinics

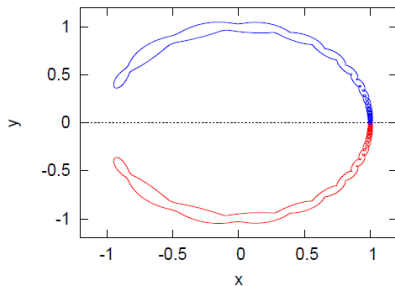


Homoclinics to Lyapunov orbits around L_3

Sun - Jupiter CRTBP - (half) horseshoe-shape homoclinics



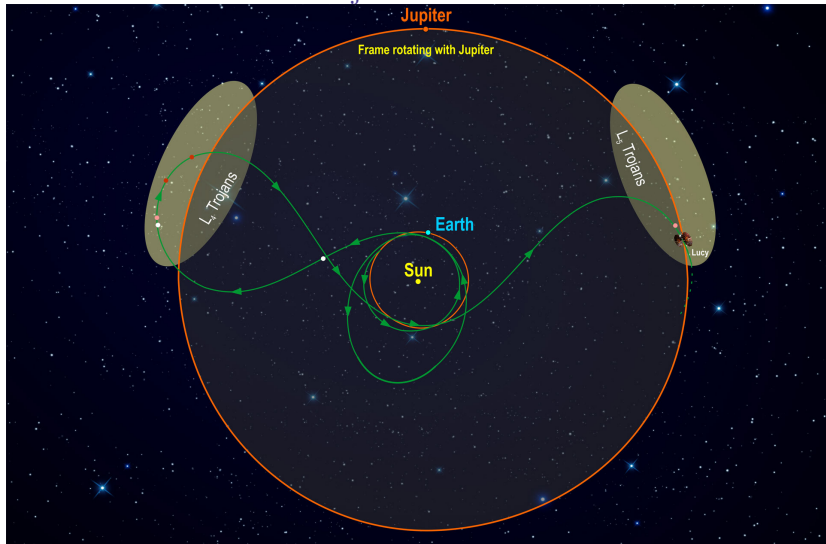
$$h = -1.49602677$$



$$h = -1.50035535$$

Horseshoe orbits are organized in families from which vertical (3d) horseshoe orbits bifurcate

Trojan Asteroids

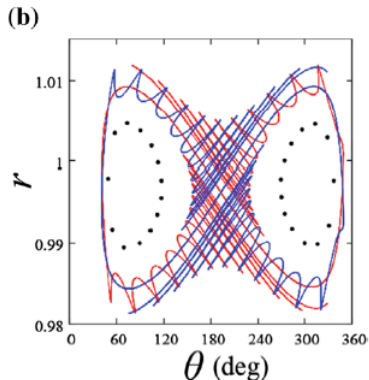
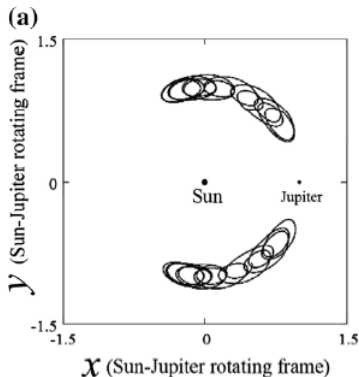


Regions of effective stability around triangular equilibrium points

- The triangular equilibrium points $L_{4,5}$ are linearly stable for $\mu < \mu_R \simeq 0.0381\dots$. Using KAM theory, \exists a dense set of invariant tori close enough to the equilibria.
- In the planar case, for each fixed energy level, the KAM tori of dimension 2 act as barriers for the dynamics. This is not true for the spatial case.
- Numerical simulations provide evidences of large regions of practical stability near $L_{4,5}$ in which the motion is non-stable but initial conditions take a long time to escape
- There is numerical evidence on the role of the centre-unstable and centre-stable manifolds of the collinear point L_3

Jumping Jupiter's Trojans

Sun–Jupiter RTBP. Poincaré section $\dot{r} = 0$ (Sun centered polar coord. (r, θ))

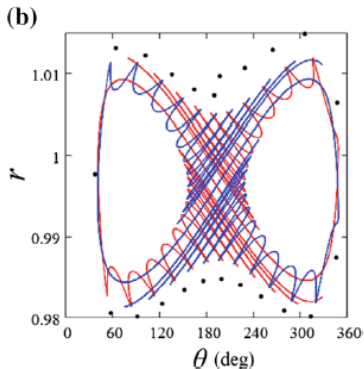
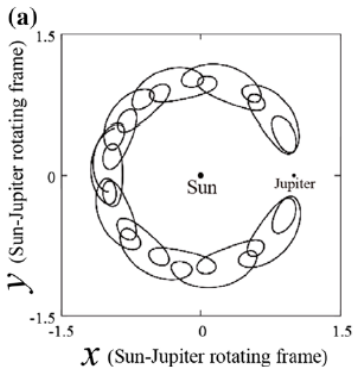


Tadpole orbits and $W^{u/s}(OL_3)$ (Lyapunov planar orbit around L_3)

Credits: Oshima, Yanao, Cel.Mech.Dyn.Astr. (2015)

Jumping Jupiter's Trojans

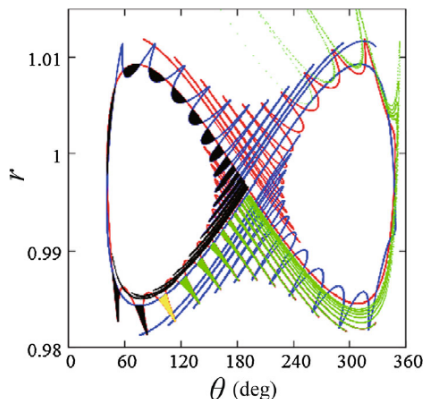
Sun–Jupiter RTBP. Poincaré section $\dot{r} = 0$ (Sun centered polar coord. (r, θ))



Horseshoe orbit and $W^{u/s}(OL_3)$ (Lyapunov planar orbit around L_3)

Credits: Oshima, Yanao, Cel.Mech.Dyn.Astr. (2015)

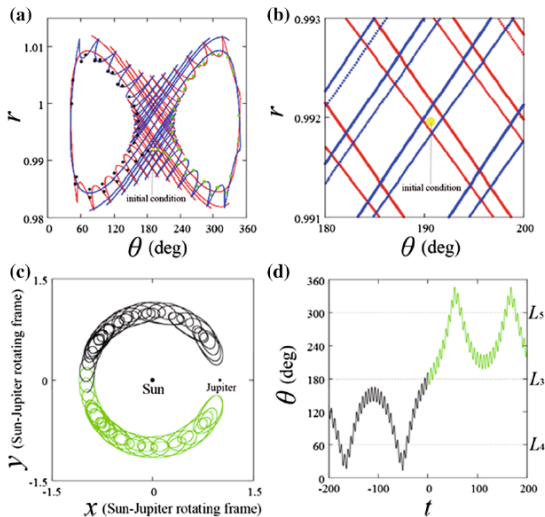
Jumping Jupiter's Trojans



Regions of escape from and capture into (forwards or backwards) the vicinity of L_4 through a neighborhood of L_3

Credits: Oshima, Yanao, Cel.Mech.Dyn.Astr. (2015)

Jumping Jupiter's Trojans



Outline

Introduction

A paradigmatic model

The circular RTBP

Invariant manifolds

Other manifolds

Interplanetary networks

Space mission design

Natural phenomena

Other models

Bicircular

Parabolic

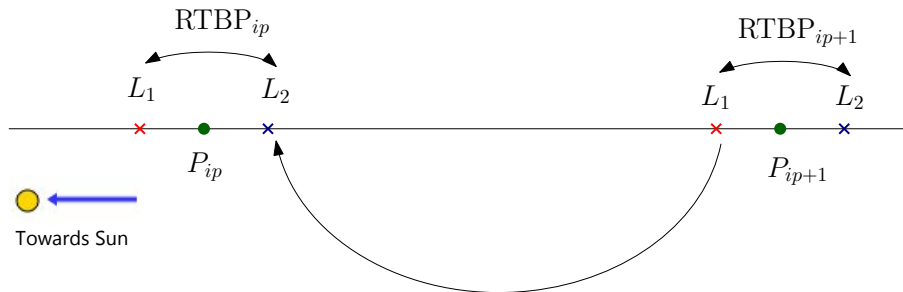
Other models

Remember that all models are wrong; the practical question is how wrong do they have to be to not be useful.

George E. P. Box (1918–2013)

Short-time mass transport

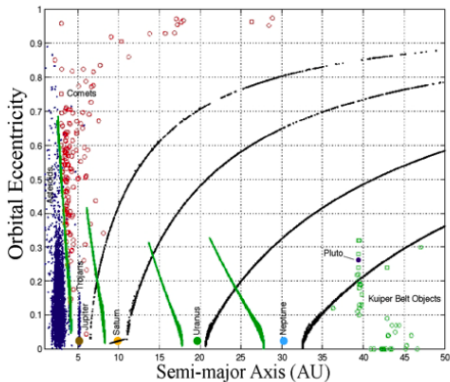
Short-time transport is based on the \exists of **pseudo-heteroclinic** connections between libration point orbits of **uncoupled** pairs of consecutive CRTBP



Scheme of the chain of connections between two consecutive Sun-Planet CRTBP

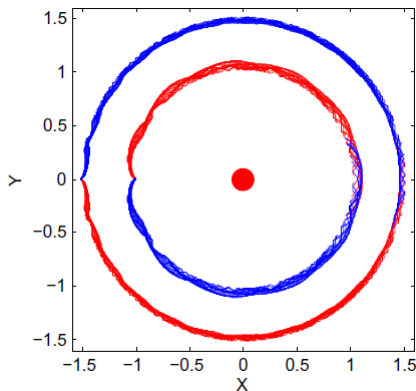
Short-time mass transport

Osculating orbital elements of the 1-dimensional invariant manifolds $W^u(L_2)$ and $W^s(L_1)$ of the collinear libration points L_1 and L_2 in a chain of CRTBP



Credits: Lo, Ross, Tech. Report. (1999)

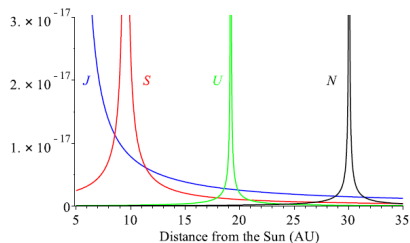
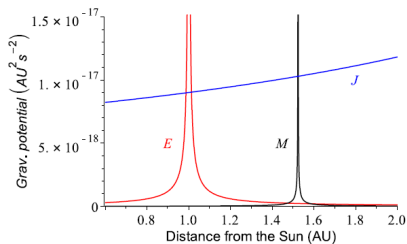
Short-time mass transport



Branches of stable (blue) and unstable (red) invariant manifolds of p.o. around L_1 in the Sun–Mars and L_2 in the Sun–Earth CRTBP. In “short-time”, they do not intersect.

Credits: Y.Ren, M.Masdemont, G. Gómez, E.Fantino, *Commun. Nonlinear Sci Numer. Simulat.* (2012)

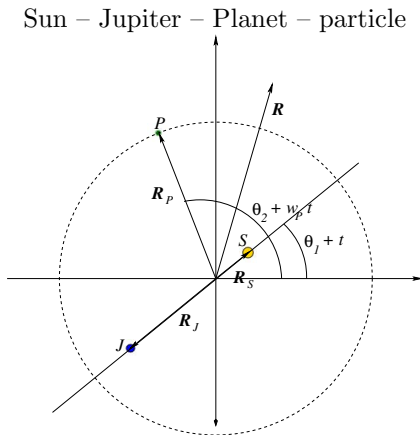
Gravity potential in the Solar System



Values of the gravity potential (in AU^2s^{-2}) of the: (LEFT) **Earth**, **Mars** and **Jupiter** up to 2 AU and (RIGHT) **Jupiter**, **Saturn**, **Uranus** and **Neptune** in the outer Solar System

Bicircular Restricted Four Body Problem (BR4BP)

Is a periodic perturbation of the CRTBP that includes the gravitational effect of a third primary on the particle.



Bicircular Restricted Four Body Problem (BR4BP)

Is a periodic perturbation of the CRTBP that includes the gravitational effect of a third primary on the particle.

$$H = \frac{1}{2}(p_x^2 + p_y^2 + p_z^2) - xp_y + yp_x - \frac{1-\mu}{r_1} - \frac{\mu}{r_2} - \frac{\mu_P}{r_P} + \frac{\mu_P}{a_P^2}(y \sin \theta + x \cos \theta)$$

$$r_1 = ((x - \mu)^2 + y^2)^{1/2},$$

$$r_2 = ((x - \mu + 1)^2 + y^2)^{1/2},$$

$$r_P = ((x - a_P \cos \theta)^2 + (y - a_P \sin \theta)^2)^{1/2},$$

$$\theta = \theta_2 - \theta_1 + t(\omega_P - 1),$$

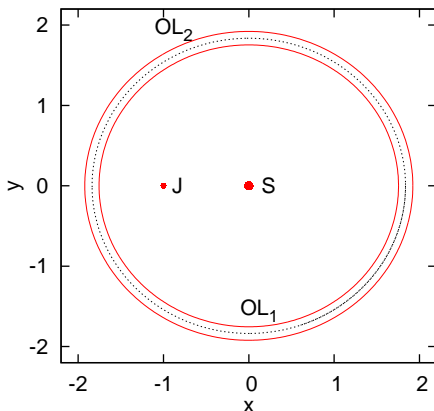
$$\mu = \frac{m_J}{m_J + m_S},$$

$$\mu_P = \frac{m_P}{m_J + m_S}$$

$$\omega_P^2 a_P^3 = 1 + \mu_P$$

Dynamical substitutes in the BR4BP

The equilibrium points L_i of the Sun-Planet CRTBP are replaced by periodic orbits.



Projection in configuration space (rotating coordinates) of the dynamical substitutes

(JSDC 2019) OL_1 and OL_2 (orbit of the planet in a dotted line)

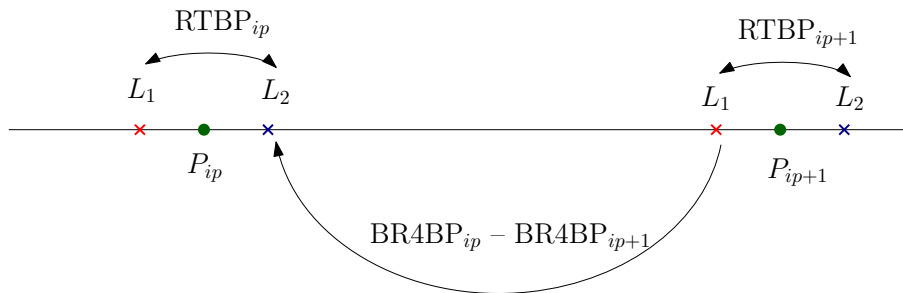
Dynamical substitutes in the BR4BP

The dynamical substitutes OL_i inherit the hyperbolicity.

Outer planets	$\Lambda(OL_i), i = 1, 2$	Inner planets	$\Lambda(OL_i), i = 1, 2$
Neptune	3.492, 3.286	Mars	$9 \times 10^7, 2.5 \times 10^8$
Uranus	14.105, 12.473	Earth	$2.8 \times 10^7, 3.4 \times 10^7$
Saturn	$6.5 \times 10^4, 2.5 \times 10^4$	Venus	$1.5 \times 10^7, 1 \times 10^7$

Value of the eigenvalue $\Lambda > 1$ corresponding to the dynamical substitutes $OL_i^{iP}, i = 1, 2$ of each bicircular problem.

Mass transport: chain of BR4BP

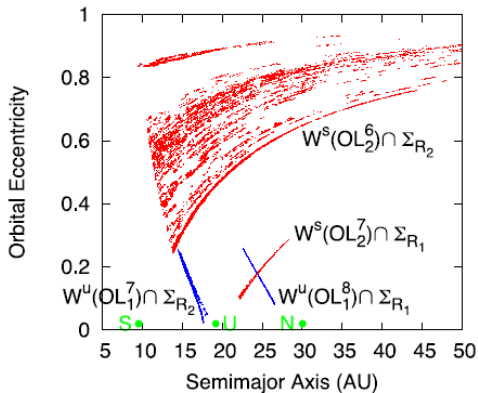


Chain of the models: Sun-Jupiter-Planet $_{ip}$ – Sun-Jupiter-Planet $_{ip+1}$

$$W^s(OL_2^{ip}) \cap W^u(OL_1^{ip+1})$$

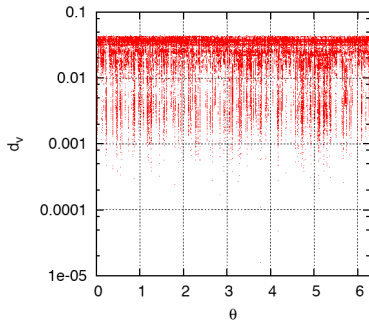
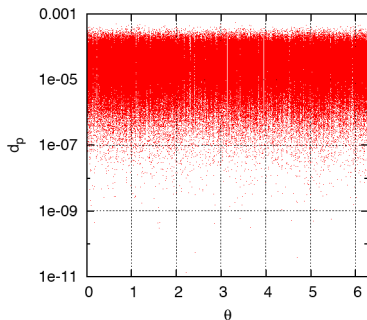
Mass transport: chain of BR4BP

Osculating semimajor axis vs eccentricity for the points (at a given section) of $W^u(OL_1^8)$ and $W^u(OL_1^7)$ (in blue), and $W^s(OL_2^7)$ and $W^s(OL_2^6)$ (red)



Mass transport: chain of BR4BP

The invariant manifolds $W^s(OL_2^{ip})$ and $W^u(OL_1^{ip+1})$ are followed up to a intermediate section $R = \text{const.}$ to look for intersections. When there is a match in position, Δv is measured



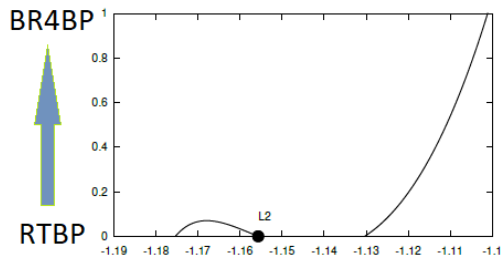
Minimum distances d_p (positions, left) and d_v (velocities, right) between points of the invariant manifolds at the section Σ_{R_1} of the Uranus and Neptune bicircular problems

The BR4BP: yes and no

- The BR4BP can be a **good model**
 - to explore the intersection of the $W^{u/s}(OL_{1,2})$ in a chain of bicircular models for the outer Solar System to explain mass transport. Only **linear approximation** of $W^{u/s}$ and **short time** ($10\,000 \times$ period Jupiter) has been taken into account. Better approximations and longer times could improve the results and give intersections, even for the inner planets.
 - for the study of the vicinity of the triangular points $L_{4,5}$ of the main two bodies (two regions of effective stability).

The BR4BP: yes and no

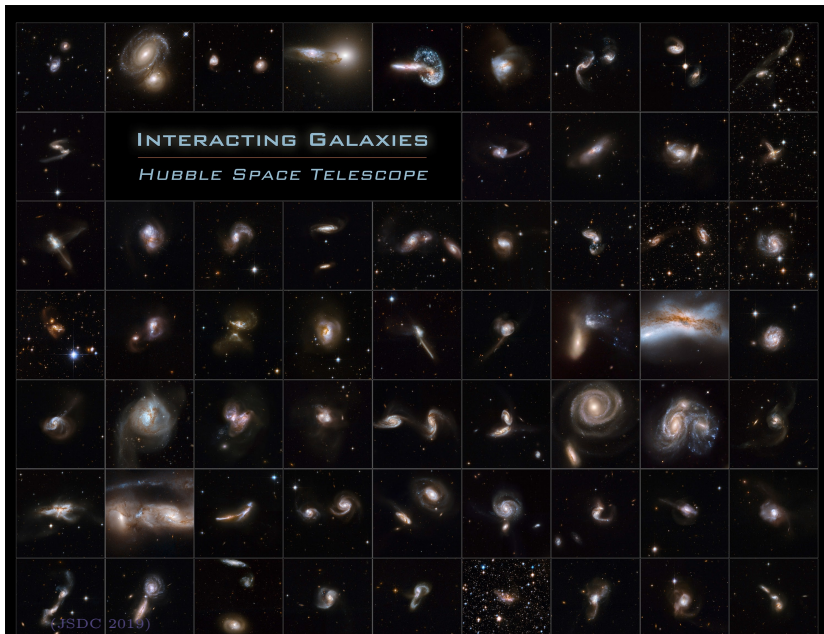
- The BR4BP **is not useful** for the study of the the translunar point in the Earth-Moon-Sun-particle system.



Credits: M. Jorba. PhD Thesis. (2019)

The BR4BP: yes and no

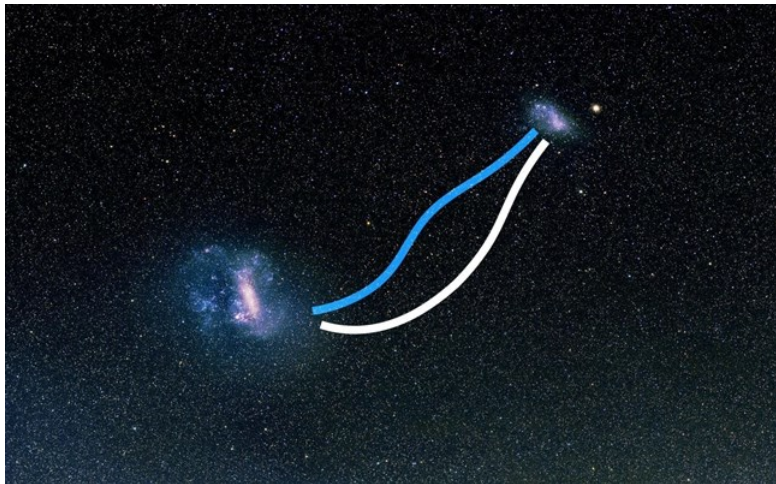
- The BR4BP **is not a coherent model**: the primaries does not verify Newton's laws. The Quasi-Bicircular Problem is a coherent version of the BR4BP: needs the computation of a quasi-bicircular solution of the three body problem.
- The Solar Radiation Pressure can be included in both the BR4BP and the Quasi-Bicircular model





Galaxies NGC 3808A (right) and NGC 3808B (left).

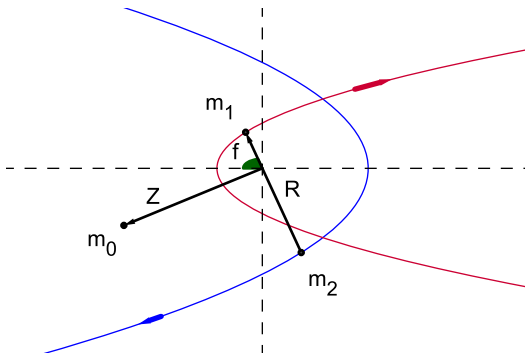
Credits: NASA, Hubble Space Telescope (2015)



Magellanic system

Credits: Belokurov et al. MNRAS (2017)

The Planar Parabolic Restricted Three-Body Problem



$$\frac{d^2 \mathbf{Z}}{dt^2} = -(1 - \mu) \frac{\mathbf{Z} - \mathbf{Z}_1}{|\mathbf{Z} - \mathbf{Z}_1|^3} - \mu \frac{\mathbf{Z} - \mathbf{Z}_2}{|\mathbf{Z} - \mathbf{Z}_2|^3},$$

The Planar Parabolic Restricted Three-Body Problem

Compatification to extend the flow when $s \rightarrow \pm\infty$: $\sin(\theta) = \tanh(s)$.

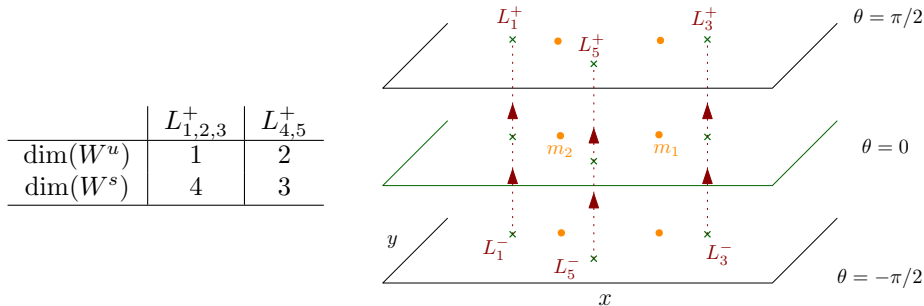
$$\left\{ \begin{array}{l} \frac{d\theta}{ds} = \cos \theta, \\ \frac{d\mathbf{z}}{ds} = \mathbf{w}, \\ \frac{d\mathbf{w}}{ds} = -A(\theta)\mathbf{w} + \nabla\Omega(\mathbf{z}) \end{array} \right. \quad A(\theta) = \begin{pmatrix} \sin \theta & 4 \cos \theta \\ -4 \cos \theta & \sin \theta \end{pmatrix},$$

$$\Omega(\mathbf{z}) = x^2 + y^2 + 2 \frac{1 - \mu}{\sqrt{(x - \mu)^2 + y^2}} + 2 \frac{\mu}{\sqrt{(x - \mu + 1)^2 + y^2}}.$$

$\theta = \pm\pi/2$ are invariant \rightarrow Boundary problems (infinity)

The Planar Parabolic Restricted Three-Body Problem

10 equilibrium points at the boundaries of the phase space that correspond to “infinity”: $L_{1,2,3}^{\pm}$, collinear points, $L_{4,5}^{\pm}$ triangular points



	$L_{1,2,3}^+$	$L_{4,5}^+$
$\dim(W^u)$	1	2
$\dim(W^s)$	4	3

The $W^s(L_i^+)$ and $W^u(L_i^-)$, $i = 1, 2, 3$ are of **co-dimension 1**.

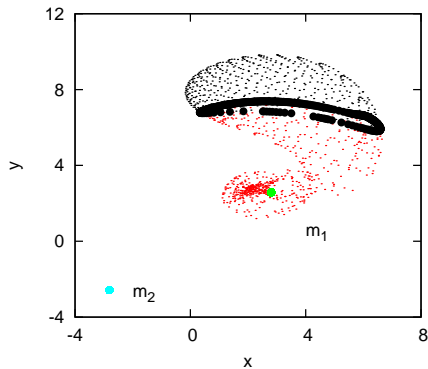
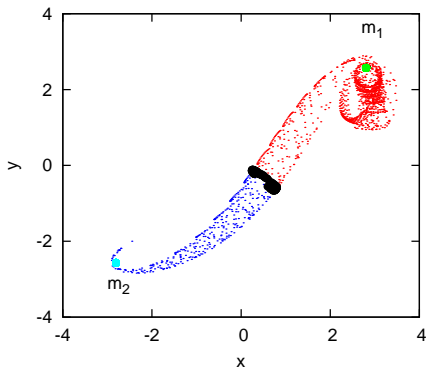
Generating bridges and tails

Dynamics forwards in time:

- There exist of only two different types of final evolutions: **capture orbit** (around a primary) or **escape orbit** (far away from both primaries).
Collision manifolds: $W^{u/s}(m_j)$.
- The invariant manifolds $W^u(L_{1,2,3}^-)$ and $W^s(L_{1,2,3}^+)$ are of codimension 1: they behave as a frontier and divide the phase space in regions where only one of the two final evolutions are allowed: escape or capture.
- Heteroclinic connections between the equilibrium points and the collision manifolds:

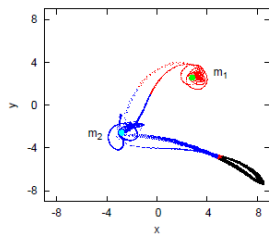
$$W^s(L_i^+) \cap W^u(m_j), \quad i = 1, 2, 3 \quad j = 1, 2$$

Bridges and Tails

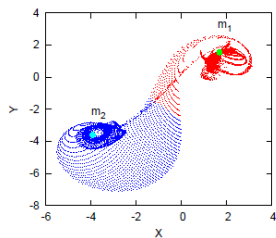


$$\mu = 0.5$$

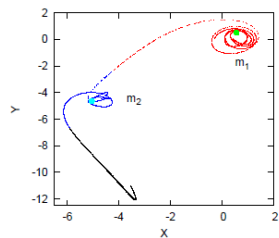
Bridges and Tails



$\mu = 0.5$



$\mu = 0.3$



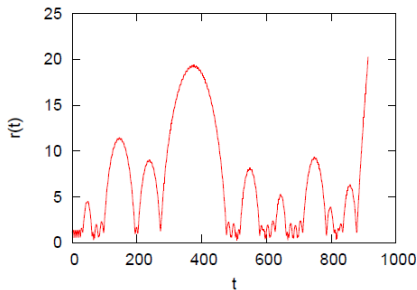
$\mu = 0.1$

Atomic dynamics

The same methodologies/ideas can be applied to atomic (classic) dynamics:

- ionization in a hydrogen atom in a circularly polarized microwave field

$$H = \frac{1}{2}(p_x^2 + p_y^2) - (xp_y - yp_x) - \frac{1}{r} + Kx$$

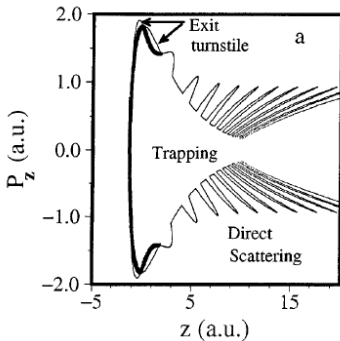
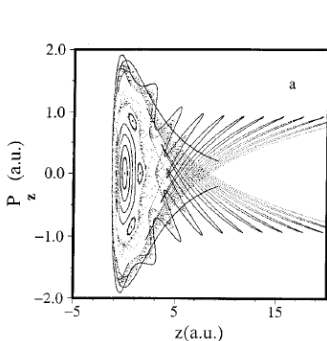


Atomic dynamics

The same methodologies/ideas can be applied to atomic (classic) dynamics:

- the scattering of the ${}^4\text{He}$ from different Cu surfaces

$$H = \frac{1}{K}(p_x^2 + p_z^2) + V(x, z)$$



Credits: Borondo, Guantes, Phys. Rev. E (1997)

Thank you for your attention